Studying the effects of ACCVD grown CNTs on physical and microstructural behaviors of Stellite-6/CNTs nanocomposite

GHUZANFAR SAEED[a, *], FAZAL AHMAD KHALID[a], MUHAMMAD TARIQ SAEED CHANI[b], MUHAMMAD UMER FAROOQ[a], IRFAN H. ABIDI[a], TAHIR SATTAR[a]
[a]*Faculty of Materials Science and Engineering, GIK Institute of Engineering Sciences and Technology, Topi (23640), KPK, Pakistan*
[b]*Chemistry Department, Faculty of Science, King Abdulaziz University, Jeddah 21589, Saudi Arabia*

ACCVD grown CNTs were used for the fabrication of nanocomposites via powder metallurgy technique. Varied wt. % of CNTs (0.5, 1, 1.5 and 2) was used in nanocomposites development. Effects of varied CNTs wt. % on the physical, microstructural and phase behaviors of nanocomposites were the main investigating objectives of this study. Relatively density of Stellite-6/CNTs nanocomposites varied with the increase of CNTs wt. %. As for as the microstructural aspects of nanocomposites are concerned, detailed optical and SEM analyses were performed. Through optical microstructure analyses, a region named as Stellite-6/CNTs composites was prominent for the nanocomposites materials as compared to plain material. SEM analyses confirmed the denser microstructures of nanocomposites with the increase of CNTs wt. %. CNTs sustained and no any unwanted phases were detected for Stellite-6/CNTs nanocomposite material after high temperature sintering process.

(Received September 9, 2014; accepted August 3, 2016)

Keywords: Alcoholic Catalytic Chemical Vapor Deposition (ACCVD), Carbon Nanotubes (CNTs), Powder Metallurgy (PM), Relatively density, Metallic Nanocomposites (MN)

1. Introduction

Since the discovery of carbon nanotubes in 1991 [1], carbon nanotubes (CNTs) have attracted attention to create new materials and devices for a variety of applications due to their remarkable physical, mechanical, chemical and electronic properties [2-4]. Addition of carbon nanotubes to matrix material as a reinforcement has led to the development of advanced nanocomposites materials with superior mechanical properties as compared to the conventional composite materials [5-6]. There are three well-known techniques described to synthesize carbon nanotubes [7-9]; e.g. electric arc, laser ablation and chemical vapor deposition. Among these techniques, CVD is considered better because of its simplicity in operation, high yield of CNTs, low operational cost and low temperature reaction [10-12].

The chemical vapor deposition process provides an opportunity to use carbon precursor in liquid, solid or gaseous form for the growth of carbon nanotubes [13]. Previous work [14] reported synthesis of high quality SWCNTs using liquid precursor (methanol and ethanol) over Fe-Co catalysts supported on zeolite. Another study was also successful in the synthesis of high quality SWCNTs by alcoholic decomposition over catalyst powder using CVD method [15]. Synthesis of CNTs over conducting glass, nickel plates and porous alumina substrates is accomplished using Fe and Co acetates as catalyst by ethanol decomposition [16]. Further investigation in the synthesis of high quality MWCNTs over pre-deposited Fe-catalyst thin film was carried out by ethanol decomposition [17]. The results of carbon nanotubes synthesized by ethanol decomposition showed better quality owing to OH^- radicals that are beneficial for the removal of amorphous carbon and other impurities [14, 18]. Fe, Co and Ni based nano-catalyst particles are beneficial in the growth of CNTs. As Stellite-6 is a Co based alloy and it was used for CNTs growth for various ACCVD reaction times. Detail described in our other study [19].

Stellite-6 alloy possesses good mechanical and oxidation resistances [20-21] which are important for wear and high temperature applications in both cases (bulk and coating materials). Possible applications of Stellite-6/CNTs nanocomposites may be for the development of hard alloy nano composite/coatings materials.

It was found that no systematic study has been conducted on the fabrication of Stellite-6/CNTs nanocomposites via powder metallurgy technique. CNTs used as reinforcing agents as described before were grown via ACCVD method at FMSE/GIKI laboratories. There were three main objectives of this study: as to investigate the effects of varied wt. % of grown CNTs on the physical, microstructural and phase behaviors of Stellite-6/CNTs nanocomposites.

2. Experimental details

For the fabrication of Stellite-6/CNTs nanocomposites, different wt. % of grown CNTs e.g. 0.5, 1, 1.5 and 2 were added as reinforcing agents in Stellite-6 matrix material. Nanocomposites were fabricated via powder metallurgy technique. Green compacts of Stellite-6/CNTs nanocomposites were sintered at 1250 °C for three hours and then were cooled to room temperature at cooling rate of 15 °C/min. Theses sintered plain and nanocomposites materials were further carried to study the impact of varied wt. % of CNTs on physical, macro/micro-structural and phase behaviors of Stellite-6/CNTs nanocomposites. Relative densities of fabricated materials were measured by taking ratios between experimentally and theoretical measured densities. For the study of microstructures, some optical (Olympus B061 microscope, Japan) and SEM (JEOL, JED-2300 Analysis station, Japan) analyses were performed. Phase analyses for fabricated nanocomposites were performed by using STO-German X-Ray diffraction equipment. All the samples before and after sintering process were scanned between 20 to 80 2θ° with a step size of 0.04/sec at 25°C.

3. Results and discussion

Experimental densities of green plain Stellite-6 and other nanocomposites compacts were calculated by general approach (d=m/v) and theoretical densities of these materials were measured by eq. (2). Relative densities % of all these green compacts (before sintering process) were calculated by eq. (1). Relative density of plain Stellite-6 alloy has been minimum as shown in Fig. 1(a) because of its green form. Addition of increased weight % CNTs from 0.5 to 2 in the matrix of Stellite-6 alloy has increased the relative densities of nanocomposites as shown in Fig. 1 (a) but up to a critical wt. % of CNTs. After that those relative densities values have deteriorated.

$$\text{Relative density } \% = \frac{\text{green density}}{\text{theoretical density}} \times 100 \qquad (1)$$

$$\text{d composites} = \text{dm} \times \text{Vm} + \text{df} \times \text{Vf} \qquad (2)$$

After sintering cycle, the experimental densities of plain and Stellite-6/CNTs nanocomposites were measured by Archimedes principle and the theoretical densities were calculated by eq. (2). Relative densities % of sintered materials were calculated by using eq. (3). There are number of reasons which have increased the relative densities % of sintered Stellite-6/CNTs nanocomposites compacts (0.5, 1, 1.5 and 2 wt. %) as compared to green compacts (Fig. 1a); e.g. sintering process which caused densification. Densification process resulted in porosity reduction. Furthermore, densification of nanocomposites was also improved due to increased wt. % of CNTs (Fig. 4). As higher wt. fraction of reinforcing particulates filled open pores more effectively.

$$\text{Relative density } \% = \frac{\text{sintered density}}{\text{theoretical density}} \times 100 \qquad (3)$$

We have observed the gradual reduction in the relative densities % for both green and sintered (Fig. 1a & b) fabricated Stellite-6/CNT nanocomposites after a critical 1.5 wt. % of CNTs. Added CNTs are always located on grain boundaries [22]. CNTs located at grain boundaries were beneficial up to a critical wt. % to make nanocomposites denser. After that these have reduced the relative densities. Possible reasons for the reduction in the relative density % for higher 2 wt. % of CNTs are lower grains packing factor due to agglomeration phenomena of ACCVD grown CNTs.

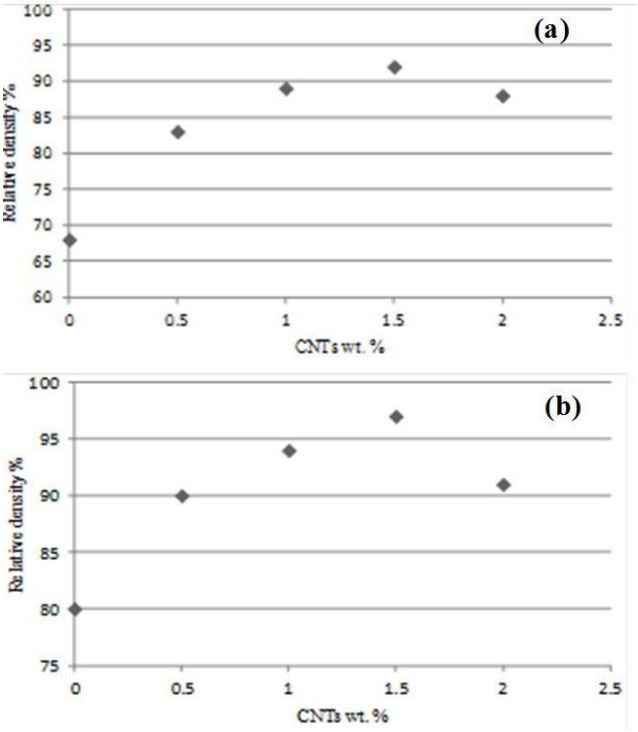

Fig. 1. Variation of relative densities (a) before and (b) after sintering process with varied CNTs wt. %

Some macro level analyses were performed before and after high temperature sintering process for Stellite-6/ 1 wt. % CNTs nanocomposites and the results are demonstrated in Fig. 2 (a) and (b) respectively. In comparison, it is very clear that there were differences in compacts diameter dimensions before and after sintering process. A noticeable percentage changes in diameter of the sintered samples are reported here. Diameter percentage expansion was approximately 2.941%. This demonstrated that sintering process caused densification and has resulted in porosity reduction of the sintered compact. Similar observations were also presented by G. Goudah et al. [23] in their studies. Grain growth has resulted in increased compact diameter [24-25]. Besides this, we did not notice any macro level defect like holes,

porosity and cracks for sintered Stellite-6/ 1 wt. % CNTs nanocomposites compact (Fig. 2b).

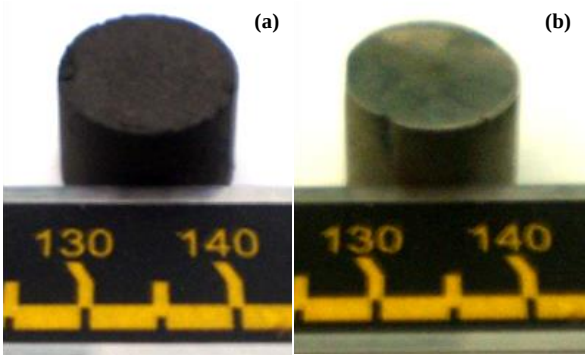

Fig. 2. Macro analyses for Stellite-6/ 1 wt. % CNTs compacts (a) before and (b) after sintering process

Optical results are shown in Fig. 3 with varied CNTs wt. % (0.5, 1, 1.5 and 2) for fabricated Stellite-6/CNTs nanocomposites. As shown in Fig. 3 (a) that very weekly bonded stellite-6 matrix grains are prominent (very openly voids can be seen clearly between grains). These results may be due to conventional pressure-less sintering. This result may different for some advance sintering techniques e.g.

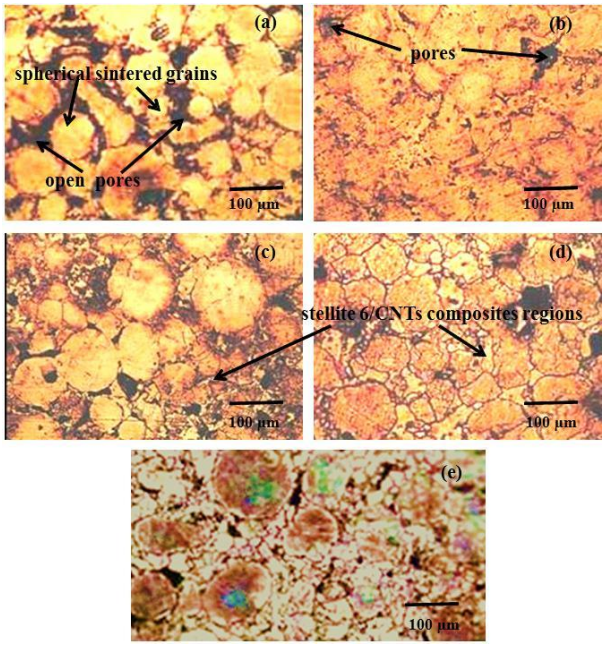

Fig. 3. Optical microscopy images: (a) Plain Stellite-6, (b) Stellite-6/ 0.5 wt. % CNTs, (c) Stellite-6/ 1 wt. % CNTs, (d) Stellite-6/ 1.5 wt. % CNTs and (e) Stellite-6/ 2 wt. % CNTs nanocomposites

Spark Plasma Sintering (SPS). Furthermore, these results also coincide with lower relative density % values of plain sintered compact (Fig. 1b). But with the increase of CNTs wt. % (Fig. 3b-e), matrix grains have bonded strongly and these appeared more uniform as well. As it is also demonstrated in these images, that voids have reduced in their sizes with the increase of CNTs wt. % (denser images). There are many valid reasons to argue for these results e.g. the presence of CNTs between matrix grains and the sintering process. CNTs filled open voids between grains and sintering process [24-25] which always promote grains growth. These both gap filling factors helped in the improvement of nanocomposites densities. CNTs reside on the grain boundaries. This was confirmed by very prominent regions named Stellite-6/CNTs nanocomposites (Fig. 3c-d).

Stellite-6 alloy exhibits a hypoeutectic microstructure with the primary FCC Co rich dendrites. Co dendrites are surrounded by Cr rich M_7C_3 eutectic carbides. For detailed microstructure of fabricated nanocomposites, SEM analyses were performed and the results are displayed in Fig. 4. In Fig. 4 (a), some very irregular bonded matrix grains are visible. Besides their poor bonding integrity, very large holes are also prominent. These present lower and inferior densification results. More importantly, no Stellite-6 phases are visible and prominent. With the addition of CNTs, Stellite-6 phases (Fig. 4b) start to manage themselves in some regular appearance. With further addition of increased wt. % of CNTs, Stellite-6 phases start to become very prominent in their appearances (Fig. 4c-e). These phases concede with literature [26-27] reported Stellite-6 phases. Pores in their sizes and volumes have reduced with the addition of higher wt. % of CNTs. This was confirmed by the presence of very small and minor sized voids (Fig. 4c-e). Reduction in sizes of pores and sever sintering conditions have helped matrix phases to be denser and systematic in their appearances.

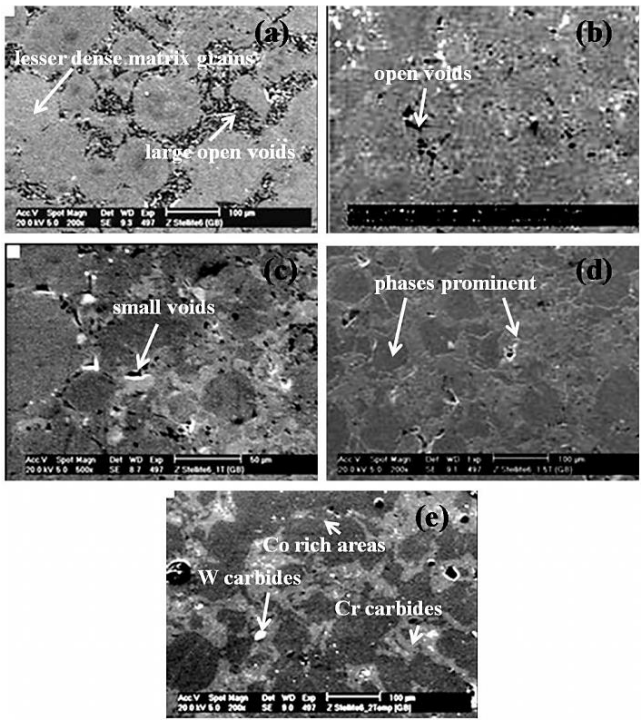

Fig. 4. Scanning Electron Microscopy (SEM) images: (a) Plain Stellite-6, (b) Stellite-6/ 0.5 wt. % CNTs, (c) Stellite-6/ 1 wt. % CNTs, (d) Stellite-6/ 1.5 wt. % CNTs and (e) Stellite-6/ 2 wt. % CNTs nanocomposites

Phase analyses were also performed for plain sintered Stellite-6 and Stellite-6/CNTs nanocomposites materials and the results are shown in Fig. 5. Phase analyses show the presence of added CNTs phase. The CNTs peaks appear at 2-theta position of 25, 41, 43 and 73. It was concluded that both MWCNTs and SWCNTs have sustained high temperature sintering reaction conditions and there was reported no any deteriorated phase. CNTs peaks became prominent and wider with the increase of CNTs wt. % from 0.5 to 2.

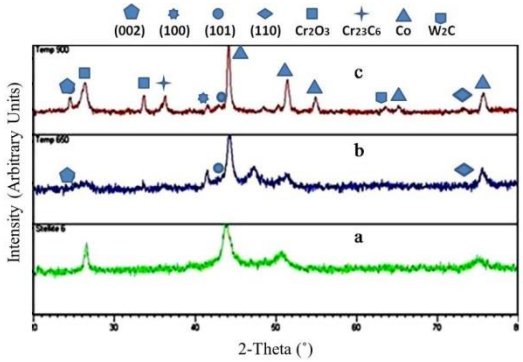

Fig. 5. Phase studies after sintering process for (a) Plain Stellite-6, (b) Stellite-6/ 0.5 wt. % CNTs and (c) Stellite-6/ 2 wt. % CNTs nanocomposites

Other common phases among plain sintered Stellite-6 and Stellite-6/CNTs nanocomposites are Cr_2O_3 and F.C.C solid solution of Co [26-27]. Cr_2O_3 appeared at 2-theta positions of 26.5. While, F.C.C solid solution of cobalt appeared at-2 theta positions of 43.5, 52, 55 and 75.5.

4. Conclusions

Stellite-6/CNTs nanocomposites were successfully fabricated via powder metallurgy technique. There were different parameters of these nanocomposites under consideration e.g. relative densities %, macro/micro structural and phase changes behaviors after sintering process. Sintering cycle has improved the densities of nanocomposites but added CNTs were effective up to a critical 1.5 wt. % and after that densities value have degraded in both cases (green and sintered). The expansion in diameter of sintered nanocomposites compact was around 2.941 %. There were some interesting micro-structural aspects of nanocomposites with increase of CNTs wt. %. Through optical analyses, stellite-6/CNTs composites regions were prominent. Voids/pores also reduced in their sizes with the increase of CNTs wt. %. SEM analyses showed that matrix phases start to become prominent with the increase of CNTs wt. %. Matrix phases like Co and W/Cr carbides were clear in their appearance for maximum wt. % of CNTs. CNTs sustained high temperature sintering conditions and no any deteriorated phases were reported.

Acknowledgments

Authors acknowledges Faculty of Material Sciences and Engineering, GIKI for providing research facilities.

References

[1] S. Iijima, Helical microtubules of graphitic, Nature **354**, 56 (1991).
[2] N. Zhao, Q. Cui, C. He, C. Shi, J. Li, H. Li, X. Du, Materials Science and Engineering A **460–461**, 255 (2007).
[3] M. Caplovicova, L. Caplovic, D. Buc, P. Vinduska, J. Janık, Journal of Electrical Engineering **61**, 373 (2010).
[4] N. Zhao, C. He, Z. Jiang, J. Li, Y. Li, Materials Letters **60**, 159 (2006).
[5] J. P. S. Delmotte, A. Rubio, Carbon **40**, 1729 (2002).
[6] J. Salvetat, J. Bonard, N. Thomson, A. Kalik, L. Forro, W. Bnoit, Appl. Phys. A **69**, 255 (1999).
[7] X. Chen, R. Wang, J. Xu, D. Yu, Micron **35**, 455 (2004).
[8] Y. Murakami, Y. Miyauchi, S. Chiashi, S. Maruyama, Chemical Physics Letters **374**, 53 (2003).
[9] I. Stamatin, A. Morozan, A. Dumitru, V. Ciupina, G. Prodan, J. Niewolski, H. Figiel, Physica E **37**, 44 (2007).
[10] O. Guellati, S. Detriche, M. Guerioune, Z. Mkhalif, J. Delhalle, Int. J. Nanoelectronics and Materials **3**, 123 (2010).
[11] K. Raji, S. Thomas, C. B. Sobhan, Applied Surface Science **257**, 10562 (2011).
[12] E. Terrado, M. Redrado, E. Munoz, W. Maser, A. M. Benito, M. T. Martinez, Material Science and Engineering C **26**, 1185 (2006).
[13] M. Kumar, Y. Ando, Journal of Nanoscience and Nanotechnology **10**, 3739 (2010).
[14] S. Maruyama, R. Kojima, Y. Miyauchi, S. Chiashi, M. Kohno, Chemical Physics Letters **360**, 229 (2002).
[15] A. Okamoto, H. Shinohara, Carbon **43**, 431 (2005).
[16] G. O. Cervantez, G. R. Morales, J. O. Lopez, Microelectronics Journal **36**, 495 (2005).
[17] M. Wienecke, M. Bunescu, K. Deistung, P. Fedtke, E. Borchartd, Carbon **44**, 718 (2006).
[18] C. Pan, Y. Liu, F. Cao, J. Wanga, Y. Ren, Micron **35**, 461 (2004).
[19] G. Saeed, M. U. Farooq, Optoelectron. Adv. Mat. **7**(9-10), 707 (2013).
[20] Y. Birol, Materials Science and Engineering A **527**, 1938 (2010).
[21] H. Kashani, A. Amadeh, H. M. Ghasemi, Wear **262**, 800 (2007).
[22] K. Kondoh, T. Threrujirapapong, H. Imai, J. Umeda, B. Fugetsu, Journal of Nanomaterials 1-4 (2008).
[23] G. Goudah, F. Ahmad, O. Mamat, Journal of Engineering Science and Technology **5**, 272 (2010).
[24] E. Neubauer, P. Angerer, G. Korb, Electronics technology. In Meeting the challenges of Electronics Technology Progress 272-277 (2005).
[25] W. M. Daoush, Powder Metallurgy and Metal Ceramics **47**(9-10), 531 (2008).
[26] H. Yu, R. Ahmed, Journal of Tribology **131**, 011601 (2009).
[27] A. Kusmoko, D. Dunne, H. Li, International Journal of Current Engineering and Technology **4**, 32 (2014).

*Corresponding author: ghznfrsd190@hotmail.com